INTERNATIONAL JOURNAL OF HYDROGEN ENERGY 42 (2017) 25877–25881

Available online at www.sciencedirect.com

ScienceDirect

journal homepage: www.elsevier.com/locate/he

Short Communication

A solid state thermogalvanic cell harvesting low-grade thermal energy

Linlin Yang, Hai Sun, Suli Wang, Luhua Jiang, Gongquan Sun *

Division of Fuel Cell & Battery, Dalian National Laboratory for Clean Energy, Dalian Institute of Chemical Physics, Chinese Academy of Sciences, Dalian 116023, China

ARTICLE INFO

Article history:
Received 24 January 2017
Received in revised form
16 August 2017
Accepted 17 August 2017
Available online 20 September 2017

Keywords:
Thermogalvanic cell
Fuel cell
Low-grade heat
Thermal energy to electrical energy conversion

ABSTRACT

A high performance polymer electrolyte thermogalvanic cell, which converts thermal energy to electrical energy directly, is transformed from a proton exchange membrane fuel cell. The transform is realized by connecting the anode and cathode chamber with a gas tube and filling hydrogen to both chambers. Provided a heat flux through the cell, hydrogen is consumed in the cold side and regenerated in the hot side while circulating in two chambers during operation. The Seebeck coefficient is 0.531 mV K^{-1} at a cold side temperature of 60.0 °C and the maximum power density could reach up to 20 μW cm^{-2} with a temperature difference of 15.3 °C between two electrodes.

© 2017 Hydrogen Energy Publications LLC. Published by Elsevier Ltd. All rights reserved.

Introduction

Low-grade thermal energy is abundantly available in forms of industrial waste heat, solar thermal, and geothermal. Several devices, such as thermoelectric generators [1–9], thermogalvanic cells [10–14] and electrochemical heat engines [15], have been developed for thermal to electric direct conversion. Among them, the thermogalvanic cells are electrochemically equivalent to semiconductor based thermoelectric devices. These cells are closed electrochemical systems wherein the reactants are regenerated by thermal energy from a heat source which flows through the device to a heat sink [10,16–19]. The merits of zero carbon emission, high reliability and noise-free make the thermogalvanic cells an attractive alternative for scavenging energy from low-grade heat [12,14].

A thermogalvanic cell consists of two electrodes in contact with an electrolyte [7]. When a temperature gradient is present, a voltage proportional to the entropy change of redox reaction is created. The $Fe(CN)_6^{4-}/Fe(CN)_6^{3-}$ couple in aqueous solution have been studied for a long time in thermogalvanic cells because of its high Seebeck coefficient (1.4 mV K^{-1}, one order of magnitude higher than typical semiconductor) and the large exchange current density [14,20,21]. Series connected n type ($Fe(CN)_6^{4-}/Fe(CN)_6^{3-}$) and p type ($Fe^{2+}/Fe^{3+}$) thermogalvanic element arrays were demonstrated by Maimani et al. and Zhang et al. displaying high power density and low cost [10,12]. However, it suffers from shortcoming in that

* *Corresponding author.*
E-mail address: gqsun@dicp.ac.cn (G. Sun).
http://dx.doi.org/10.1016/j.ijhydene.2017.08.111
0360-3199/© 2017 Hydrogen Energy Publications LLC. Published by Elsevier Ltd. All rights reserved.

it is inconvenient to fabricate and packaging an aqueous based thermogalvanic cell array in order to get a sufficient voltage to power the application. Although the beta-alumina ($\beta'' - Al_2O_3$) solid electrolyte based alkali-metal thermal-to-electric conversion cells (AMTECs) have been used in space-crafts with heat supplied from a radioisotope heat source [16,22], it is unsuitable for low-grade heat harvesting due to its high operating temperature (600–1200 K). Recently, Yang et al. fabricate a wearable thermogalvanic device based on gel electrolyte, demonstrating the facile integration and packaging using quasi-solid-state electrolyte [13]. Inspired by the successful application of Nafion® in the field of energy conversion, including chemical energy to electrical energy (fuel cell), kinetic energy to electrical energy (ionic polymer-metal composites) and salinity gradient energy to electrical energy (reverse electrodialysis) [3,24], we try to fabricate a proof-of-concept cell that convert thermal energy to electrical energy based on Nafion®.

Here we demonstrate a solid electrolyte thermogalvanic cell transformed from a proton exchange membrane fuel cell (PEMFC). The transform is realized by feeding hydrogen to both anode and cathode chamber and connecting the two chambers with gas tube. With a cold side temperature of 60.0 °C and a temperature difference between two electrodes of 15.3 °C, a maximum power density of 20 μW cm^{-2} is achieved.

Material and methods

MEA preparation

The electrodes were prepared using a screen painting method. Pt/C (Johnson Matthey Inc., Hispec 9100, 60 wt% Pt) were used as the catalyst for both anode and cathode. The metal loadings for both electrodes were 0.4 mg cm^{-2}. Carbon paper (TGP-H-060) with a microporous layer was used as gas diffusion layers on both anode and cathode sides. The MEA with an active area of 4.5 cm × 4.5 cm were prepared by pressing the anode and cathode on either side of a Nafion 117 membrane at 120.0 °C.

Results and discussion

The membrane electrode assembly (MEA) consists of two gas diffusion electrodes with a very thin layer of catalyst, pressed to either side of the proton exchange membrane (Nafion® 117), as shown in Fig. 1. The MEA used in this thermogalvanic cell is immersed into hydrogen atmosphere. Provided a temperature gradient is established between the two electrodes, there will be a potential difference. Upon reaction, hydrogen separates into protons and electrons at the cold electrode. Protons migrate through the ion conducting membrane to the hot side and electrons travel through the external circuit to do useful work. On the hot side, the reverse reaction occurs, with protons reduced to hydrogen by consuming electrons. Through the membrane we have a co-transport of proton and water from the cold side to the hot side. The reaction taking place at each electrode is: $\frac{1}{2}H_2 + t_w H_2O_{(1)} = H^+ + e^- + t_w H_2O_{(2)}$ where t_w is the transference number of water.

The driving force for the thermogalvanic cell is the transport of entropy from the high temperature source to the low temperature sink, as is the case for any heat engine [17]. The open circuit potential across the terminals is given by Ref. [18]:

$$FdE = \frac{1}{2}S_{H_2}dT - \overline{\overline{S}}_{H^+}dT - \overline{\overline{S}}_{e^-(Pt)}dT + t_w S_{H_2O} \quad (1)$$

where S is the partial molar entropy, $\overline{\overline{S}}$ is the transported entropy, and other symbols have their usual meanings. By analogy with thermoelectric phenomena, the gradient $\frac{dE}{dT}$ is defined as Seebeck coefficient

$$\varepsilon = \left(\frac{dE}{dT_1}\right)_{T_2} = \frac{1}{F}\left(\frac{1}{2}S_{H_2} - \overline{\overline{S}}_{H^+} + t_w S_{H_2O} - \overline{\overline{S}}_{e^-(Pt)}\right) \quad (2)$$

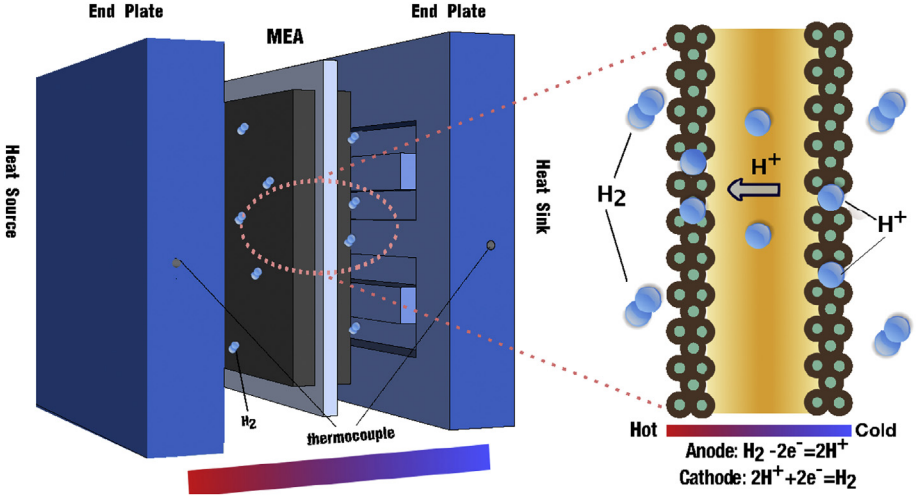

Fig. 1 – Schematic of a thermogalvanic cell. The MEA consists of a proton conducting membrane (Nafion® 117) sandwiched by two catalysed porous electrodes. The cell is filled with H_2, wherein the anode and the cathode chambers are connected together. Under a thermal gradient established by heat flow, hydrogen is consuming on the cold side and regenerating on the hot side during operation.

where T_1 is the higher temperature. As show in Eq (2), ε is temperature dependent, however, it seems probable that E can usually be represented by a linear function of temperature over a narrow range [18]. Fig. 2a shows the open circuit voltages increase linearly with the measured temperature gradient. The value of ε increases from 0.269 mV K^{-1} to 0.335 mV K^{-1} with the temperature of the cold side end plate rising from 40.0 °C to 60.0 °C. The increase in value of ε with increasing temperature is most likely due to the increased activity and conductivity of proton in Nafion® membrane.

It should be mentioned that the temperature measuring points locate in the end plates, not at the electrodes. To get the temperature difference between the two electrodes (ΔT_{MEA}), Fourier's law of heat conduction is used. At steady state, heat flow through the sections of the cells must be identical, so Fourier's law can be applied to each section as follows:

$$q = \frac{\Delta T_{MEA}}{h_{MEA}/k_{MEA}} = \frac{\Delta T_{t,c}}{R_{t,c}} = \frac{\Delta T_{plate}}{h_{plate}/k_{plate}} = \frac{\Delta T_{tot}}{\sum h/k + R_{t,c}} \quad (3)$$

where h is the thickness, k is the thermal conductivity, $R_{t,c}$ is the thermal contact resistance. According to Eq. (3)

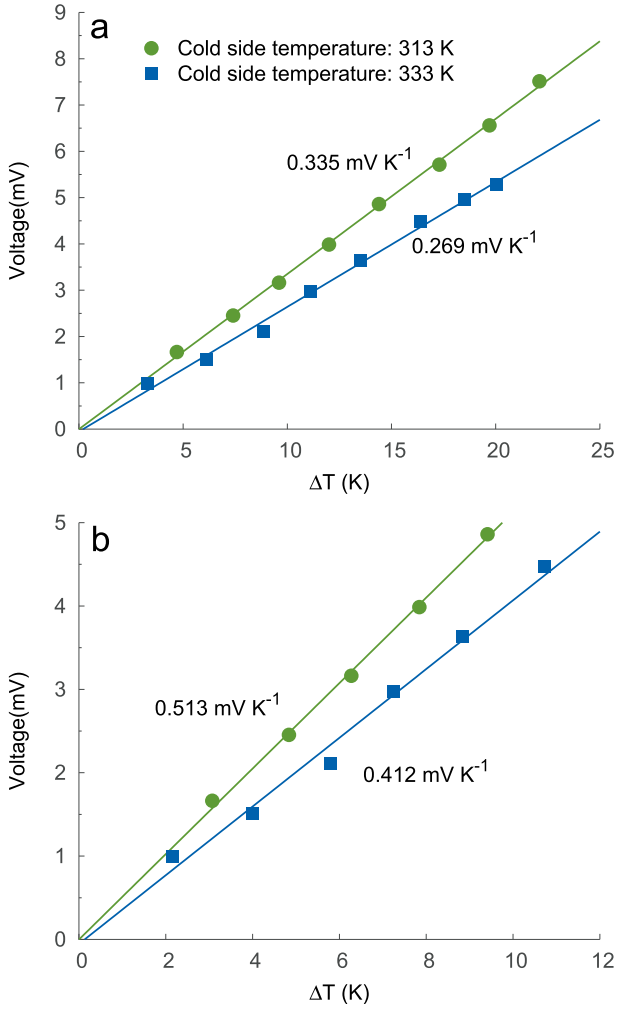

Fig. 2 – (a) Open circuit voltage versus temperature difference between end plates. (b) Open circuit voltage versus corrected temperature difference between electrodes.

$$\Delta T_{MEA} = \frac{h_{MEA}}{k_{MEA}} \frac{\Delta T_{tot}}{\sum h/k + R_{t,c}} \quad (4)$$

With the material properties given in Table 1, we get $\Delta T_{MEA} = 15.3$°C. After the temperature correction, the Seebeck coefficient are ≈1.5 times higher than that the uncorrected one, as shown in Fig. 2b.

The theoretical Seebeck coefficient can be calculated from Eq (2). The first term, S_{H_2}, i.e., the molar entropy of hydrogen gas, is 130.68 J $mol^{-1}K^{-1}$ [25]. The next two terms, $\bar{\bar{S}}_{H^+} - t_w S_{H_2O}$, i.e., the reversible entropy transferred due to the Nafion® 117 membrane, is 13.4 ± 0.2 J mol^{-1} K^{-1} at 25 °C reported by Ratkje et al. [26]. The last term, $\bar{\bar{S}}_{e^-(Pt)}$, i.e., the transported entropy of electrons in Pt, is 0.435 J mol^{-1} K^{-1} at 25 °C [18,27], thus the metallic contribution to the Seebeck coefficient is small, 4.5 μV K^{-1}. Substitution of numerical values into Eq. (2) yields ε = 0.534 mV K^{-1}. The estimation given here is close to our corrected experiment value (0.513 mV K^{-1}) at a cold side temperature of 60.0 °C.

The discharge behavior of the cell with a temperature difference of 23.3 °C between the end plates is shown in Fig. 3. The cell voltage decreases linearly in the polarization curve. Generally, there are three major types of polarization losses: (1) activation polarization losses rising from electrochemical reaction; (2) ohmic polarization losses rising from ionic and electronic conduction; (3) concentration polarization losses rising from mass transport. Hence, the slope of polarization curve (R_{slope}) represents the whole resistance (a sum of the kinetic, ohmic and mass-transport resistance). The value of R_{slope} is 721 mΩ cm^2, while the ohmic resistance of the cell determined via current interruption method by an electronic load (Arbin Instrument Corp.) is 691 mΩ cm^2. The two values are very close, indicating the performance of the cell is limited by the ohmic resistance. It is reasonable considering that the electrochemical oxidation of hydrogen on Pt surfaces and hydrogen diffusion are fast, i.e., kinetic and mass-transport losses can be neglected.

As shown in Fig. 3, with a corrected temperature difference of 15.3 °C between electrodes, i.e., a temperature difference between two end plates of 23.3 °C (cold side: 60.0 °C), a maximum power density of 20 μW cm^{-2} is achieved. For a linear i–V curve, the maximum power output is achieved at $V = \frac{1}{2}V_{oc}$ when the internal resistance (R_{int}) of the cell is equal to the external resistance:

$$P_{max} = \frac{V_{oc}^2}{4R_{int}} \quad (5)$$

Substitution of $V_{oc} = \varepsilon \cdot \Delta T$ into Eq. (5), we get

$$P_{max} = \frac{\varepsilon^2 \Delta T^2}{4R_{int}} \quad (6)$$

This means that the maximum power is proportional to ΔT^2 (assuming that ε is a constant). Hence, a normalized power density, $P_{max}/A/\Delta T^2$, is used to evaluate the performance. The cell demonstrated in this work without any optimization shows a normalized power density of 8.5 × 10^{-2}μ W $cm^{-2}K^{-2}$, as compared with 5.0 × 10^{-2} μW cm^{-2} K^{-2} reported by Hu and 5.4 × 10^{-2} μW cm^{-2} K^{-2} reported by Zhang of aqueous based thermogalvanic cell [10,14].

Table 1 – Physical parameters and properties of materials used in the cell.

	Subscript in Eq. (3)	Thickness (mm)	Thermal conductivity[a](W/m K)	Ref.
MEA	MEA	0.58	0.288	[31,32]
End plate (316L)	Plate	5 × 2	15.24	[33]
Contact resistivity		4×10^{-4} m^2 KW^{-1}		[34]

[a] Thermal conductivity is temperature dependent, but the value will not differ much in the range of 40–80 °C.

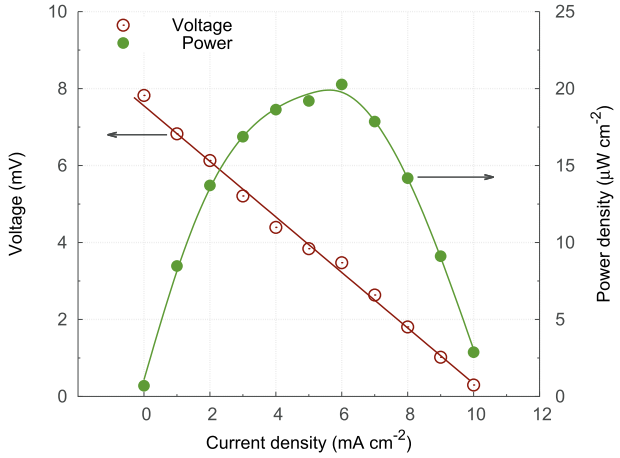

Fig. 3 – Polarization curve of the thermogalvanic cell with a cold side temperature of 60.0 °C and with a temperature difference of 23.3 °C between two end plates. The calculated temperature difference is 15.3 °C between two electrodes.

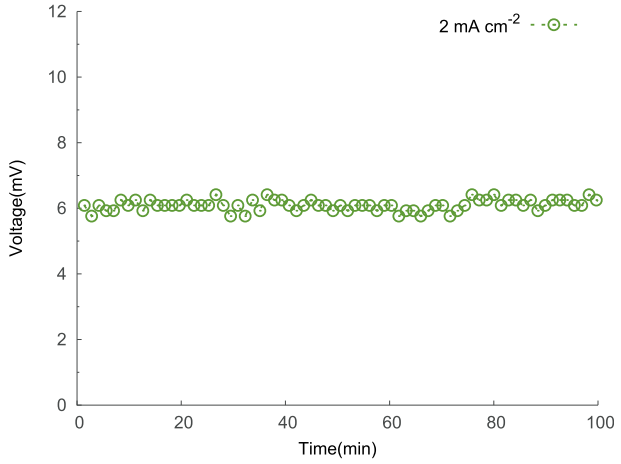

Fig. 4 – Cell voltage during steady state operation at 2 mA cm^{-2} with a temperature difference of 23.3 °C between two end plates and the cold side temperature of 60.0 °C.

The power conversion efficiency is defined as the ratio of the electrical power output divided by the thermal power flowing through the cell:

$$\eta = \frac{P_{max}}{Q} = \frac{P_{max}}{kA(\Delta T/h)} \tag{7}$$

Inserting the values of P_{max} and Q into Eq. (7), we get the efficiency of the cell relative to Carnot efficiency is 0.042%. All the low temperature thermogalvanic cells suffer from inefficiency. Presently, the efficiencies of thermogalvanic cells relative to their Carnot efficiencies are very low, ranging from *ca.* 0.001% to 4% [11,21].

Substitution of Eq. (6) and $R_{ini} = \rho(h/A)$ into Eq. (7) leads to

$$\eta = \frac{\frac{\varepsilon^2 \Delta T^2}{4\rho(h/A)}}{kA(\Delta T/h)} = \frac{\varepsilon^2 \Delta T}{4\rho k} \tag{8}$$

The figure of merit Z is defined by

$$Z = \frac{\varepsilon^2}{\rho\kappa} \tag{9}$$

Then the efficiency is proportional to Z. Although thermogalvanic cell normally have high Seebeck coefficient ε, they usually exhibit low ionic conductivity ($1/\rho$). The figure of merit, Z, is 1×10^{-5} K^{-1}, which is lower than typical values for semiconductor material (in the order of 10^{-3} K^{-1}). Considering the ion conductivity in aqueous solution and Nafion® (in the order of 10 S m^{-1}) is much lower than the electrical conductivity of best known commercially used thermoelectric material Bi_2Te_3 (4×10^4 S m^{-1}) [28], the low efficiency is attributed to the low ionic conductivity.

The durability for the thermogalvanic cell was evaluated by recording the voltage while operating at a constant temperature difference (23.3 °C) and current density (2 mA cm^{-2}). As shown in Fig. 4, the voltage is nearly constant over time, indicating a good durability of this thermogalvanic cell. Considering the MEA based on Nafion® membrane is possible to run 60000 h in PEMFC [29,30], and the operating condition for thermogalvanic cell (without oxidant O_2) is much less aggressive than that for PEMFC, the durability of this cell is expected to be much better than PEMFC.

Conclusions

In summary, we have demonstrated a thermogalvanic cell based on polymer electrolyte for harvesting low-grade thermal energy. The cell is transformed from a PEMFC by connecting the anode and cathode chamber with a gas tube and filling hydrogen to both chambers and. Provided a temperature gradient is established through the cell, hydrogen is consumed on the cold side and regenerated on the hot side while circulating in two chambers during operation. The performance of the cell is limited by the ohmic resistance and a maximum normalized power density of 8.5×10^{-2} μW cm^{-2} K^{-2} is achieved, which is competitive with aqueous based thermogalvanic cells. The solid state cell design makes this type of thermogalvanic cell a promising

device for harvesting low-grade waste-heat and environmental thermal energy.

Acknowledgement

The authors thank Bing Qin from Dalian Institute of Chemical Physics for assistance in the cell design and construction. This work is supported by the National Science Foundation of China under grant No. 21406216.

REFERENCES

[1] DiSalvo FJ. Thermoelectric cooling and power generation. Science 1999;285(5428):703–6.
[2] Sun Y, Sheng P, Di C, Jiao F, Xu W, Qiu D, et al. Organic thermoelectric materials and devices based on p- and n-type poly(metal 1,1,2,2-ethenetetrathiolate)s. Adv Mater 2012;24(7):932–7.
[3] Tsai T-C, Liu C-W, Yang R-J. Power generation by reverse electrodialysis in a microfluidic device with a nafion ion-selective membrane. Micromachines 2016;7.
[4] Hasani M, Rahbar N. Application of thermoelectric cooler as a power generator in waste heat recovery from a pem fuel cell an experimental study. Int J Hydrogen Energy 2015;40(43):15040–51.
[5] Chen Y, Chen M, Shen N, Zeng RJ. H_2 production by the thermoelectric microconverter coupled with microbial electrolysis cell. Int J Hydrogen Energy 2017;41(48):22760–8.
[6] Omer G, Yavuz AH, Ahiska R. Heat pipes thermoelectric solar collectors for energy applications. Int J Hydrogen Energy 2017;42(12):8310–3.
[7] Dupont MF, MacFarlane DR, Pringle JM. Thermo-electrochemical cells for waste heat harvesting – progress and perspectives. Chem Commun 2017;53(47):6288–302.
[8] Lu B, Meng X, Tian Y, Zhu M, Suzuki RO. Thermoelectric performance using counter-flowing thermal fluids. Int J Hydrogen Energy 2017;42(32):20835–42.
[9] Ming T, Yang W, Wu Y, Xiang Y, Huang X, Cheng J, et al. Numerical analysis on the thermal behavior of a segmented thermoelectric generator. Int J Hydrogen Energy 2017;42(5):3521–35.
[10] Zhang L, Kim T, Li N, Kang TJ, Chen J, Pringle JM, et al. High power density electrochemical thermocells for inexpensively harvesting low-grade thermal energy. Adv Mater 2017;29(12):1–7.
[11] Im H, Kim T, Song H, Choi J, Park JS, Ovalle-Robles R, et al. High-efficiency electrochemical thermal energy harvester using carbon nanotube aerogel sheet electrodes. Nat Commun 2016;7:1–9.
[12] Maimani MA, Black JJ, Aldous L. Achieving *pseudo*-'n-type p-type' in-series and parallel liquid thermoelectrics using all-iron thermoelectrochemical cells with opposite seebeck coefficients. Electrochem Commun 2016;72:181–5.
[13] Yang P, Liu K, Chen Q, Mo X, Zhou Y, Li S, et al. Wearable thermocells based on gel electrolytes for the utilization of body heat. Angew Chem Int Ed 2016;55(39):12050–3.
[14] Hu R, Cola B, Haram N, Barisci J, Lee S, Stoughton S, et al. Harvesting waste thermal energy using a carbon-nanotube-based thermo-electrochemical cell. Nano Lett 2010;10(3):838–46.
[15] Richards G, Gemmen RS, Williams MC. Solid state electrochemical heat engines. Int J Hydrogen Energy 2015;40(9):3719–25.
[16] Cole T. Thermoelectric energy conversion with solid electrolytes. Science 1983;221(4614):915–20.
[17] Chum HL, Osteryoung RA. Review of thermally regenerative electrochemical systems. Solar Energy Research Institute; 1981.
[18] Agar JN. Thermogalvanic cells. In: Delahay P, editor. Advances in electrochemistry and electrochemical engineering, vol. 3. John Wiley & Sons; 1963.
[19] Zhou H, Yamada T, Kimizuka N. Supramolecular thermo-electrochemical cells: enhanced thermoelectric performance by host-guest complexation and salt-induced crystallization. J Am Chem Soc 2016;38:10502–7.
[20] Burrows B. Discharge behavior of redox thermogalvanic cells. J Electrochem Soc 1976;123(2):154–9.
[21] Quickenden TI, Mua Y. A review of power generation in aqueous thermogalvanic cells. J Electrochem Soc 1995;142(11):3985–94.
[22] Tournier J-M, El-Genk MS. Performance analysis of pluto/express, multitube AMTEC cells. Energy Convers Manag 1999;40(2):139–73.
[24] Vinh ND, Kim H-M. Ocean-based electricity generating system utilizing the electrochemical conversion of wave energy by ionic polymer-metal composites. Electrochem Commun 2017;75:64–8.
[25] Lemmon E, McLinden M, Friend D. Thermophysical properties of fluid systems. In: NIST chemistry WebBook, NIST standard reference database number 69. National Institute of Standards and Technology; 1998. http://webbook.nist.gov.
[26] Ratkje SK, Otty M, Halseid R, Strmgrd M. Thermoelectric power relevant for the solid-polymer-electrolyte fuel cell. J Membr Sci 1995;107(3):219–28.
[27] deBethune AJ. Irreversible thermodynamics in electrochemistry. J Electrochem Soc 1960;107(10):829–41.
[28] Goldsmid HJ. Introduction to thermoelectricity. Springer; 2010.
[29] St Pierre J, Wilkinson D, Knights S, Bos M. Relationships between water management, contamination and lifetime degradation in PEFC. J New Mater Electrochem Syst 2000;3(2):99–106.
[30] Endoh E. Highly durable PFSA membranes. In: Handbook of fuel cells. John Wiley & Sons, Ltd; 2010.
[31] Burheim O, Vie P, Pharoah J, Kjelstrup S. Ex situ measurements of through-plane thermal conductivities in a polymer electrolyte fuel cell. J Power Sources 2010;195(1):249–56.
[32] Burlatsky SF, Atrazhev VV, Gummalla M, Condit DA, Liu F. The impact of thermal conductivity and diffusion rates on water vapor transport through gas diffusion layers. J Power Sources 2009;190(2):485–92.
[33] Incropera FP, DeWitt DP, Bergman TL, Lavine AS. Fundamental of heat and mass transfer. John Wiley & Sons; 2006.
[34] Khandelwal M, Mench M. Direct measurement of through-plane thermal conductivity and contact resistance in fuel cell materials. J Power Sources 2006;161:1106–15.